

CLASSICAL AND QUANTUM BILLIARDS: INTEGRABLE, NONINTEGRABLE AND PSEUDO-INTEGRABLE * †

KAROL ŻYCZKOWSKI

Instytut Fizyki, Uniwersytet Jagielloński,
ul. Reymonta 4, 30-059 Kraków, Poland

(Received January 10, 1992)

Statistical properties of the spectra of quantum two dimensional billiards are shown to be linked to the nature of the dynamics of the corresponding classical systems. Quantized pseudo-integrable billiard exhibits level repulsion, in spite of non chaotic dynamics of its classical counterpart. We conjecture that the level statistics of a quantum pseudo-integrable system depends on the genus of the invariant manifold equivalent to its classical phase space. A model of billiards with finite walls suitable to investigate the problems of chaotic scattering is proposed.

PACS numbers: 05.45.+b, 03.65.-w

1. Introduction

Classical billiards were studied for several years by mathematicians and physicists as simple dynamical systems of various interesting features. A particle bouncing on a plane between hard elastic walls exhibits different kind of dynamics depending on the shape of the billiard. Its motion is regular in a rectangular or circular billiard and the system is integrable. Two independent integrals of motion are known, the dynamics of the system is restricted to an invariant two dimensional torus and each trajectory might be predicted for arbitrary long times with arbitrary precision [1,2]. However, if a circular obstacle is put inside the rectangle (Sinai billiard) or the circle is transformed into a stadium (Bunimovich billiard) the system becomes

* Presented at the IV Symposium in Statistical Physics, Zakopane, Poland, September 19-29, 1991.

† This work has been partially supported by the project 20084-91-01 of Polski Komitet Badań Naukowych.

chaotic [3,4]. The Kolomogorov entropy of the system is positive [5] and two neighbouring trajectories in the phase space diverge exponentially in time. This feature limits a possibility of computing the long time behaviour of a trajectory starting from a given point in the phase space.

These different properties of the classical billiards exert an influence on their quantum analogues. Chaotic behaviour of the classical model manifests itself in the statistical properties of the spectrum of the corresponding quantum system [6,7]. Whereas for integrable systems the Poisson distribution of the level spacing statistics was found [7,8], the spectra of the classically chaotic systems display level repulsion and the Wigner statistics of level spacing was observed [8-11]. Interesting piece of information can also be extracted from eigenfunctions of quantized billiards. In general the classically chaotic systems produce irregular eigenstates - messy looking objects without any spatial correlations [12]. On the other hand it was shown by Heller [13] that some eigenfunctions of chaotic system display regular structures, which can be associated with classical periodic orbits. These objects, called *quantum scars* were later analyzed by numerous authors [14-17]. A theory linking the properties of spectrum of quantum system with the presence of classically unstable periodic orbits has been established [18-20], but several questions concerning the classical to quantum correspondence for chaotic systems remain still open.

In this work we focus our attention on classical and quantum billiards. Section 2 reviews main results obtained for classical integrable and chaotic billiards, while the subsequent section concerns the pseudointegrable systems [21]. In particular the billiards in rational polygons provide variety of pseudointegrable systems characterized by an integer genus g of the classical phase space $1 > g > \infty$ [22]. Such systems are nonintegrable but also non chaotic: the largest Lapunov exponent (and the Kolomogorov entropy) is not positive [23].

In Section 4 the quantized billiards are considered. We recall the statistical properties of spectra that allow to differentiate between classically regular and chaotic systems and discuss the phenomenon of quantum scars occurring for some eigenfunctions. In the next section the level statistics for simple pseudointegrable system - the "L" shape billiard is presented. In spite of the fact that the dynamics of the corresponding classical system is not chaotic, the level repulsion, typical to classically chaotic models, is observed. On the other hand, the nearest neighbour spacing distribution for this case differs significantly from the Wigner surmise and we conjecture that it depends only on the genus of the classical phase space. This hypothesis might be supported by recent measurements of the absorption spectrum of microwave resonators performed by Stöckmann and Stein [24,25].

In Section 6 we consider the billiards with penetrable walls and show

their usefulness to study chaotic scattering [26-28]. Section 7 contains concluding remarks and a list of open questions that require further investigation.

2. Classical chaotic billiards

A classical Hamiltonian system with n degrees of freedom is called integrable, if there exist n independent integrals of motion [29], and the phase space is homeomorphic with the n dimensional torus. Integrable systems are analyzed in detail in every handbook for classical mechanics and usually attract a lot of authors attention. One might think, therefore, that integrability is in some sense typical to all Hamiltonian systems. This is not the case - integrable systems are of measure zero in space of Hamiltonian systems and are so often discussed in literature only because it is relatively easier to find their solution.

A classical two dimensional billiard consists of a particle moving on a plane between reflecting walls. Dynamics of this system depends on the shape of the enclosure. Only for few particular boundaries the billiards are integrable. Some of them like rectangle, equilateral triangle or circle are depicted in figure 1. According to the Arnold theorem [29] the classical dynamics is restricted in this case to a 2-dimensional invariant torus embedded in the 4 dimensional phase space, the motion of the particle is regular and two close trajectories can diverge linearly in time. However, in the generic case, the 2-dimensional billiard is non integrable, and a typical trajectory explores 3-dimensional manifold of the constant energy. Distance between two neighbouring trajectories $D(t)$ grows exponentially in time and the largest Lapunov exponent, defined as [2]

$$\lambda = \lim_{T \rightarrow \infty} \lambda(T), \quad \lambda(T) = \lim_{D(0) \rightarrow 0} \frac{1}{T} \ln \left(\frac{D(T)}{D(0)} \right), \quad (1)$$

is positive. The Lapunov exponent λ characterizes the local instability of the classical motion, and may depend on the position of the initial point in the phase space. A billiard with trajectory with positive λ is called chaotic.

One may speculate that a billiard with a generic shape of the boundary is typically chaotic, but it is not at all simple to find a precise condition fulfilled by all chaotic billiards. In early seventies it was shown by Sinai [30] that a rectangular billiard with a circular obstacle is chaotic — see Fig. 1(b). The desymmetrised version of the system (right triangle with one edge rounded — dashed lines) owns the same dynamical properties. One eighth of the circle rounding one edge of the triangle is concave and Sinai proved that due to this dispersing fragment of the boundary the billiard becomes chaotic. This dispersing part of the enclosure plays the role of

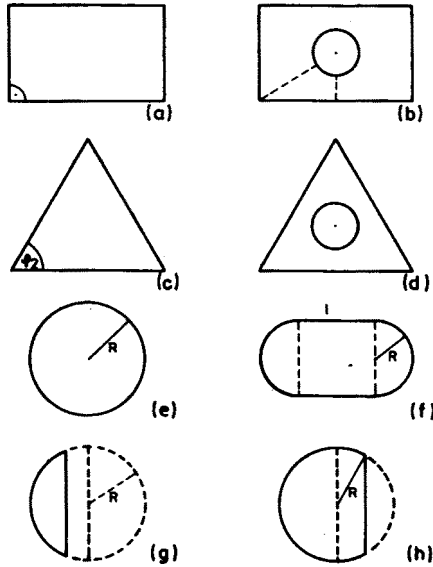


Fig. 1. Regular billiards ((a), (c), (e), (g)) and the corresponding chaotic billiards ((b), (d), (f), (h)).

the negative curvature and the mechanism of stochasticity in such systems is similar to that one present in geodesic flow on manifold with negative curvature [31]. A billiard with convex fragments is also called dispersing or hyperbolic.

The billiard in an ellipse is integrable. Lazutkin proved [32] that the caustics exists also for a slightly deformed ellipse (curvature remains smooth function of the arcs length) and the dynamics in such convex billiard is not chaotic. One could speculate, that the elliptic (convex) billiards produce stable behaviour, in contrast to the chaotic hyperbolic system of Sinai. This picture became more confusing when Bunimovich presented an evidence that the motion in the elliptic stadium billiard (Fig. 1(f)) is chaotic [4]. Moreover, he found a general rule to construct a chaotic billiard using arcs of the circle and the straight lines [33]. It occurred that the billiard in a half of a circle (or a smaller part of it - Fig. 1(g)) is regular, while a part of the circle containing its diameter (Fig. 1(h)) is chaotic. At a first glance is not easy differentiate regular and chaotic billiards even for the simplest boundaries: the Figures 1(a),(c),(e),(g) present some examples of regular systems and the Figures 1(b),(d),(f),(h) show the corresponding chaotic billiards.

A problem of finding a general principle to design billiards with positive Lapunov exponents attracts still a lot of attention. Wojtkowski found [34] a wide class of the chaotic billiards build of convex fragments of variable

curvature. For example the billiards in epicycloid, nephroid, cardioid or a square with an obstacle in the shape of an astroid are shown to be chaotic. These results have been further generalized by Markian [35] and Bunimovich [36], but the question, what condition is fulfilled by all chaotic billiards, remains still unsolved.

3. Rational polygons

The difference between the integrable and chaotic classical systems can be easily seen if one investigates the behaviour of their trajectories in the phase space. The trajectories of an integrable system are confined to an invariant manifold R which is topologically equivalent to a torus (an object with genus g equal to one), while the trajectories of a chaotic system explore the whole available phase space. There are, however, also dynamical systems, the phase space trajectories of which are bounded on invariant manifolds which are topologically equivalent to multi-handled spheres with genus $g \geq 2$. These intermediate cases, called *pseudo-integrable* were analyzed first by Zemlyakov and Katok [21]. A classical dynamics of such systems is not chaotic [22,23] (zero Lapunov exponent and Kolomogorov entropy), but the distance between two neighbouring trajectories grows quadratically in time [37]. It is due to singularities occurring in the enclosure of the billiard [38,39] like edges, corners or point interactions [40], which split a beam of trajectories into two separate parts.

In the following we shall focus our attention on the billiards with polygonal enclosures. These systems may be divided in two classes. A polygon billiard is called *rational* [23], if all angles between sides of the polygon P are rational multiples of π . The phase space trajectories are then confined to an invariant manifold R that is obtained by unfolding the original billiard [38].

Let P be a rational polygon with vertex angles $\pi n_i/m_i$, $i = 1, \dots, k$ and let M be the least common multiple of the integer denominators m_i . Each trajectory in a rational polygon can take at most $2M$ different directions after all successive collisions [41]. This stands in contrast to the dynamics in an irrational billiard where the number of directions explored by a single trajectory is infinite. The invariant manifold R of the rational billiard P consists of $2M$ copies of the initial polygon. Identifying the corresponding opposite sides of R one gets a surface of genus g (a 'pretzel' with g holes), where [22,23]

$$g = 1 + \frac{M}{2} \sum_{i=1}^{i=k} \frac{n_i - 1}{m_i}. \quad (2)$$

One immediately sees that g equals to unity for all integrable billiards depicted in Fig. 2(a): rectangle, equilateral triangle and triangles with an-

gles equal to $\pi/3, \pi/2, \pi/6$ and $\pi/2, \pi/4, \pi/4$. Polygon R has in these cases the shape of rectangle, parallelogram or regular hexagon and is (after identification of the opposite sides) topologically equivalent to a torus shown in Fig. 2(b).

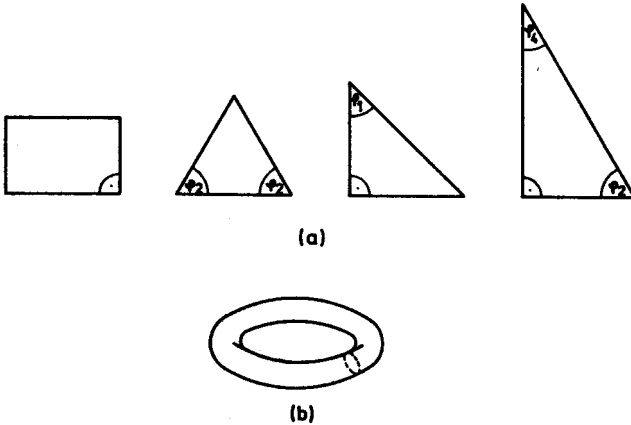


Fig. 2. (a) Integrable billiards in polygons; (b) the corresponding manifold of genus 1 - torus. The angles in all pictures are equal $\varphi_1 = \pi/4$, $\varphi_2 = \pi/3$, $\varphi_3 = 2\pi/3$, $\varphi_4 = \pi/6$, $\varphi_5 = 5\pi/6$, $\varphi_6 = \pi/5$.

A simple example of genus 2 billiard is the gnomon and, if it is symmetric, also its half. Many other examples are known: the rhombus with vertex angle equal to $\pi/3$, or, in general, a $\pi/3$ parallelogram; the triangles with the angles $(2\pi/3, \pi/6, \pi/6)$, $(3\pi/5, \pi/5, \pi/5)$, $(\pi/2, 3\pi/8, \pi/8)$, the deltoids with angles $(2\pi/3, \pi/3, 2\pi/3, \pi/3)$ and $(3\pi/4, \pi/4, 3\pi/4, \pi/4)$ or the trapeze $(\pi/2, \pi/2, \pi/3, 2\pi/3)$. Some of them are presented in Fig. 3(a), while the Fig. 3(b) represents the topology of the genus 2 manifold R . Each orbit is instantaneously moving on one torus (like in a regular system) but may skip to the other coupled torus. These changes of the torus occur in an erratic way and are responsible for certain degree of randomness in the dynamics of the pseudointegrable system.

The genus 3 is characteristic for $\pi/4$ parallelogram or for a billiard in the shape of 3 rectangular steps (an additional "step" added to the gnomon). Also the triangles $(3\pi/8, 3\pi/8, \pi/4)$, $(\pi/7, \pi/7, 5\pi/7)$, $(\pi/8, 2\pi/8, 5\pi/8)$, $(\pi/3, \pi/9, 5\pi/9)$, a rectangle with the right triangle cut away along one side or the trapeze $(\pi/2, \pi/2, 5\pi/6, \pi/6)$ (Fig. 4(a)) lead to dynamics on a 'tree holes' object represented in Fig. 4(b).

Some examples of $g = 4$ billiards like $\pi/5$ rhombus, $2\pi/3$ hexagon and $\pi/3$ arrow are displayed in Fig. 5(a). Moreover, in agreement with the

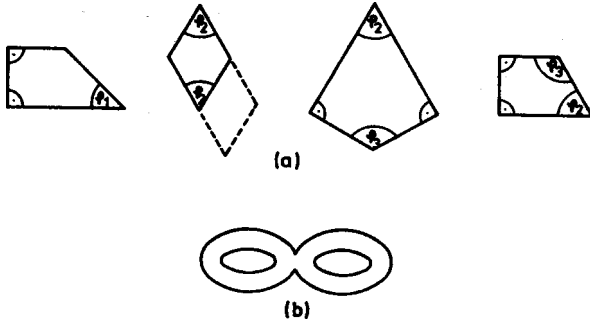


Fig. 3. (a) Billiards in polygons of genus 2; (b) and the manifold topologically equivalent to the phase space.

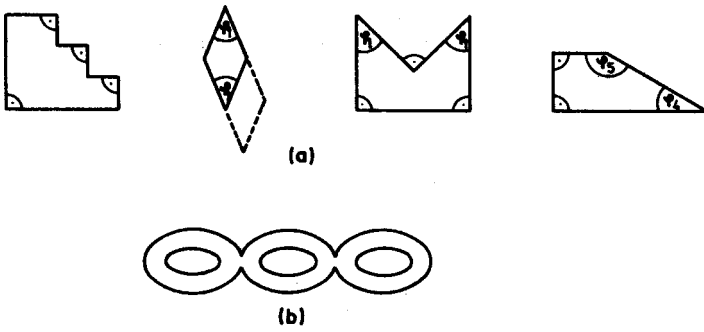


Fig. 4. As in Fig.3 for genus 3.

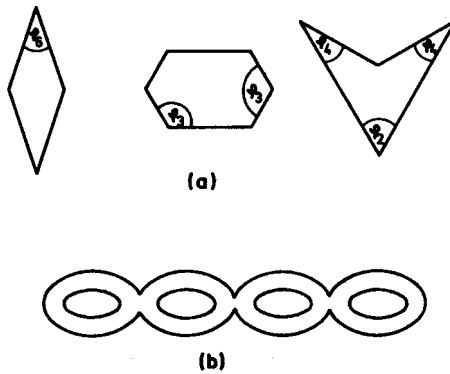


Fig. 5. As in Fig.3 for genus 4.

equation (2), the rhombus with vertex angle equal to $\pi/(N + 1)$ or the N -steps rectangular staircase (Fig. 6(a)) correspond to manifolds of genus $g = N$ sketched in Fig. 6(b). Knowing examples of billiards belonging to each of the classes labeled by the finite genus g one can study the transition between rational and irrational billiards [41,42].

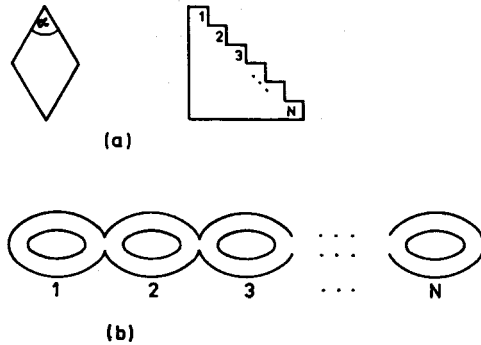


Fig. 6. (a) Scheme of billiards in polygons of genus N ; (b) and the manifold topologically equivalent to the phase space.

This approach was applied in [41] where a system consisting of the rhombus with various vertex angles $\beta = n\pi/m$ have been studied with the ratio $\nu = \beta/\pi = n/m$ being the successive rational approximations of the golden mean. The genus characterizing such system grows with the denominator m and tends to infinity for irrational billiards. The topological structure of the phase space becomes then more complicated what influences the character of the classical dynamics. It has been conjectured that the irrational billiards (the limiting case) typically allow for the ergodic motion [23], but no rigorous prove have been found. The classical pseudointegrable billiards can be thus considered as the intermediate case manifesting some features of both integrable and chaotic systems.

4. Quantized billiards

Let us consider a point particle moving in the two dimensional infinite potential well

$$V(x, y) = \begin{cases} 0, & \{x, y\} \in \Omega \\ \infty, & \{x, y\} \notin \Omega \end{cases} \quad (3)$$

where the compact set Ω is determined by the shape of the classical billiard $\partial\Omega$. In order to analyze the corresponding quantum system one needs to

solve the stationary Schrödinger equation, which in this case reduces to the Helmholtz equation

$$(\nabla^2 + k^2)\psi(x, y) = 0 \quad (4)$$

with the Dirichlet boundary condition $\Psi(x, y) = 0|_{\{x, y\} \in \partial\Omega}$. For the integrable billiards presented in Fig. 2(a) this can be done analytically [43,44], where in all other cases the numerical calculations are necessary [12,22,45].

As it has been discussed in Section 2 the classical dynamics depends strongly on the shape of the billiard and can be characterized by the largest value of the Lapunov exponent. Since the classical trajectory loses its meaning in quantum mechanics the concept of the Lapunov exponent (1) can not be easily generalized for quantum mechanics. Some progress in this matter has already been achieved [46,47], but instead of analyzing the time evolution of quantum wave packets it is far more convenient to investigate the statistical properties of the set of eigenvalues of the stationary Schrödinger equation.

Let $\{E_0, E_1, E_2, \dots\}$ denotes the infinite sequence of the eigenvalues and $\{\phi_0, \phi_1, \phi_2, \dots\}$ the corresponding sequence of the eigenfunctions of the equation (4). According to the Weyl formula [48] the mean spacing between levels of the quantum billiard $\bar{s} = \langle E_{i+1} - E_i \rangle$ is in the first approximation inversely proportional to the area of the billiard Ω . Further corrections to this formula take into account the specific features of the billiard's enclosure like corners and edges [48].

Defining the scaled spacing by $s_i := (E_{i+1} - E_i)/\bar{s}$ it is useful to study the probability distribution $P(s)$ for a given system. It has been demonstrated [7,8] that for the classically integrable systems the level spacing distribution is given by

$$P_p(s) = e^{-s}. \quad (5)$$

The above distribution is called *Poisson*, since it describes the statistics of random numbers obtained in the Poisson Process. In other words the levels of a typical regular system (harmonic oscillator is not generic!) do not display any correlations and behave like random numbers. Poisson distribution (5) is represented by a solid line in Fig. 7. The largest probability occurs for small spacing s and it is probable to find two levels close together. This property is called *level clustering*. Numerical investigation of a generic integrable billiard (rectangle with incommensurate sides) proved [44] that its level spacing distribution is close to Poissonian. This property is not restricted to the integrable billiards only, but is universal for classically regular systems [8].

The level spacing distribution for classically chaotic systems displays quite different behaviour exhibiting the *level repulsion* ($P(s \rightarrow 0) \rightarrow 0$). Numerous studies of various chaotic systems [6,8-12,49-52] showed that the

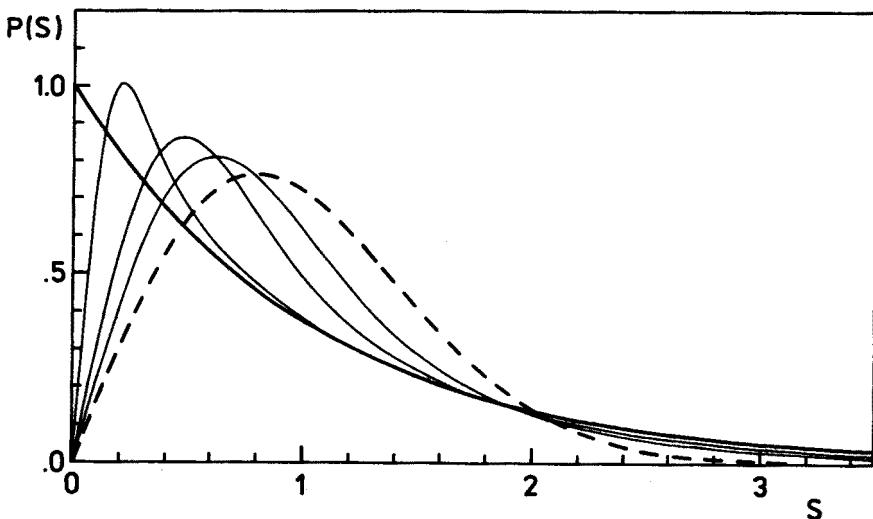


Fig. 7. Level spacing distribution $P(s)$ - bold line represents Poisson, dashed line Wigner distributions and three faint lines result from additive ensemble with coupling parameter $\lambda = 0.1, 0.3$ and 0.5 .

level statistics may be described by ensembles of random matrices [53,54]. For chaotic systems possessing the time reversal symmetry the *Gaussian Orthogonal Ensemble* (GOE) is applicable [55]. It consists of symmetric matrices build of random Gaussian numbers with zero mean and the variance inversely proportional to the matrix size N . The GOE level spacing distribution, obtained in the limit $N \rightarrow \infty$, might be well approximated by the *Wigner surmise*, received for 2×2 matrices [56,57]

$$P_W(s) = s \frac{\pi}{2} e^{-s^2 \pi/4}. \quad (6)$$

The accuracy of this approximation is sufficient to analyze a set of, say, 10^4 eigenvalues. For much larger samples, however the difference between the numerical data and the Wigner formula (6) becomes visible [58].

The above distribution, represented by a dashed line in Fig. 7, displays linear level repulsion: for small spacing $P(s) \sim s^\beta$; $\beta = 1$. For systems without generalized time-reversal symmetry, like billiards in magnetic field [59] the *Gaussian Unitary Ensemble* (GUE) should be applied and the quadratic level repulsion $\beta = 2$ was reported for Aharonov-Bohm billiards [60] and periodically kicked top [61].

Magnetic field also may change the properties of regular billiards. The billiard in an ellipse becomes chaotic for sufficiently strong perpendicular magnetic field [62]. In this case only a fraction b of the classical phase space

is occupied by a chaotic layer. Fair approximation of the level spacing distribution was proposed by Berry and Robnik [63] by superposition of two independent spectra corresponding to regular and chaotic systems. The obtained family of distributions is labeled by the parameter b ranging from 0 (Poisson distribution) and 1 (Wigner distribution).

Another family of distributions can be obtained by a composition of two ensembles of random matrices [64,65]. Consider an ensemble H_λ composed of the diagonal random matrices with Poisson spectrum H_0 and the GOE member G

$$H_\lambda = c(H_0 + \lambda G), \quad (7)$$

where the coefficient $c = (1 + \lambda^2)^{-1/2}$ is introduced to keep all eigenvalues in a bounded energy range [65]. For $\lambda = 0$ one starts with the Poisson distribution obtaining GOE spectrum in the limit $\lambda \rightarrow \infty$. In the simplest case of 2×2 matrices the resulting level spacing distribution $P_\lambda(s)$ can be expressed in terms of the Tricomi function [65]. Moreover, recent numerical investigation proved [66] that it is also suitable for large matrices pertaining to the additive ensemble H_λ . Three cases of this distribution obtained for $\lambda = 0.1$, $\lambda = 0.3$ and $\lambda = 0.5$ are represented by faint lines in Fig. 7. In contrast to the Berry Robnik formula for arbitrary small positive values of λ $P_\lambda(0) = 0$ and the linear level repulsion occurs $P_\lambda(s) \sim ts$. The slope t decreases with a growing parameter λ and in the limiting case $\lambda \rightarrow \infty$ approaches the value $\pi/2$ characteristic to the Wigner distribution.

Several other families of distributions interpolating between Poisson and Wigner were found [67-70] and applied for investigation of various quantum chaotic systems. Interestingly the Brody distribution [67] provides good approximation of the level spacing distribution received for different systems, in spite of the fact that there is no physical arguments supporting this choice. The GOE level distribution seems to be universal for quantum chaotic systems, with an exception of the composite, elongated billiards or systems like the quantum kicked rotator, where the dynamical localization occurs. On the other hand the transition from regular to chaotic motion (or from localization to delocalization) has not any universal properties and is system dependant.

Apart of level spacing distribution, measuring the distribution of distances between neighbouring levels it is appropriate to analyze the *number variance* $\Sigma^2(L)$ (average variance of the number of states in an interval containing on average L levels) or the *spectral rigidity* $\Delta_3(L)$ [71,55]. These quantities take into account higher correlations between eigenvalues and are associated to the dynamics of the corresponding classical model. For regular systems both measures grow linearly with L [72]. On the other hand for chaotic systems, described by GOE, the spectral rigidity grows as

$\Delta_3 \sim \ln(L)$ [60]. This property is universal for small values of L , while for $L > L_c$ the discrepancies from the above prediction are observed [73]. The critical value L_c is determined by the period of the shortest periodic orbit and obviously depends on the system. Moreover, fluctuations of the spectral rigidity Δ_3 and the number variance Σ^2 for large values of L may be explained by the existence of classical periodic orbits [74]. These features, specific to each particular chaotic system, cannot be described by the theory of random matrices and universal ensembles.

In a classically chaotic system the unstable periodic orbits are of measure zero and their presence does not change the global properties of the classical dynamics. On the other hand, the quantization can enhance role of some of the periodic orbits and they may significantly influence the quantum dynamics. They manifest themselves not only in the specific properties of the spectrum (fluctuations of the density of the spectrum [18] and the spectral rigidity [73]) but also affect some eigenstates of a quantum system. In contrast to regular and organized eigenfunctions of integrable quantum systems, the eigenstates of classically chaotic systems are usually irregular and their nodal lines form an erratic pattern [12]. The values of the wave function behave like a Gaussian random variable (with the zero mean and the variance inversely proportional to the area of the billiard [12]), the *path correlation function* of such eigenstate decays to zero and exhibits random fluctuations [75] and the *spatial correlation function* is isotropic and oscillates with the displacement length $|s|$ like the Bessel function $J_0(|s|)$ [12]. These quantitative description makes it possible to differentiate precisely between regular and chaotic wave functions.

This simple picture has been changed when Heller found [13] that also some eigenstates of the chaotic stadium billiard display easily recognizable regular structures caused by classical periodic orbits and exhibit space correlations different to those predicted for irregular states. Such objects, detectable in the plot of a given eigenstate $|\phi_n(x, y)|^2$ as increased density of probability, are called *quantum scars* [13,14], and might be regarded as fingerprints of the classical dynamics. The semiclassical theory of quantum scars has been developed [15,76] providing an approximation for the wave function, averaged over a small energy interval. Recently it has been suggested [16,17] to investigate quantum scars not only in the configuration space but in the phase space as well. The Wigner [16] or Husimi [17,77,78] distributions of the eigenstate aid to associate a given scar with the periodic orbits responsible for localization.

Even though this approach proved to be successful, the fundamental question what eigenstates are at all scarred, still waits for its answer. Furthermore one may address a question what eigenstates are scarred by a given periodic orbit Γ . Let us construct a coherent state $\Psi_A(0)$ localized

in the vicinity of a phase space point A that generates the periodic orbit Γ . Already the expansion of Ψ_A in the complete basis of eigenfunctions ϕ_n allows us to find relevant eigenstates yielding considerable scalar product $a_l = |\langle \Psi_A | \phi_l \rangle|^2$. The corresponding eigenvalues E_l label eigenstates scarred by the analyzed periodic orbit Γ [79]. In order to work directly in the energy domain let us consider the time evolution $\Psi_A(t)$ of the initially coherent wave packet. Defining the autocorrelation function

$$C(t) = \langle \Psi_A(0) | \Psi_A(t) \rangle, \tag{8}$$

we pass to the energy domain by the Fourier transform

$$|W(\omega)| = \left| \int C(t) \exp(-i\omega t) dt \right|.$$

The function $|W(\omega)|$ provides an important piece of information: its peaks indicate the energy intervals containing scarred eigenfunctions. This approach has been effectively applied to a simple time dependent system — periodically kicked top [79]. The semiclassical approximation of the propagator and autocorrelation function does not allow to locate a single scarred eigenstate, however, it marks the quasienergy range where scarring is most probable. Analogous method may be also applied to study the scarring phenomenon in quantized billiards, particularly using the technique of semiclassical approximation of the autocorrelation function developed recently for the stadium billiard by Tomsovic and Heller [80].

Having computed numerically several eigenstates ϕ_n of a considered system one may select the scarred states simply by analyzing the probability density $|\phi_n(x, y)|^2$. In order to define quantitatively the the degree of scarring it has been proposed [81,82] to integrate the density along each periodic orbit Γ_r . The quantity

$$I_r^n := \frac{S}{L} \oint_{\Gamma_r} |\phi_n(x, y)|^2 ds \tag{9}$$

measures the localization of the eigenstate ϕ_n along the orbit Γ_r and the prefactor normalizes the mean value of I_r^n to unity. Here L stands for the length of the orbit, S denotes the area of the billiard and the integration variable $ds = (dx^2 + dy^2)^{1/2}$.

Defined above quantity I_r^n is useful to state whether n -th eigenfunction is scarred by a given periodic orbit Γ_r [81], but does not help to answer the more general question, if a particular eigenstate is at all scarred. One may compute the space correlation function or the distribution of the wave function values and compare the numerical results with the predictions obtained

theoretically for irregular states [12] treating considerable discrepancies as an evidence of scarring. This method, however, does not provide any information, what periodic orbit is responsible for the detected scars. To compromise both goals we suggest to analyze the eigenstates in the momentum representation

$$\phi_n(k_x, k_y) = \frac{1}{2\pi} \int dx \int dy \phi_n(x, y) \exp[-i(k_x x + k_y y)].$$

Working in radial coordinates $k_x = k \cos(\theta)$, $k_y = k \sin(\theta)$, we define for each eigenstate the angular distribution function

$$F_n(\theta) = \int_0^{\infty} |\phi_n(k, \theta)|^2 k dk. \quad (10)$$

The function $F(\theta)$ has a simple interpretation as the probability distribution of angles in the momentum space. For a classical periodic orbit in a billiard consisting of K segments the function F consists of, at most, $2K$ singular lines in the range $\theta \in [0, 2\pi)$ (the time-reversal symmetry is assumed). Their positions on the θ axes are determined by the angles explored by the orbit and their relative heights are proportional to the total length of the segments laying at the selected angles. The sequence of these lines is characteristic to each periodic orbit: knowing the classical angular distribution $F(\theta)$ one may uniquely point the appropriate periodic orbit or its associates. In the opposite case of a classical ergodic trajectory the angular distribution is continuous (all possible angles are explored) and fluctuates around its mean value $\langle F \rangle = 1/2\pi$.

The integrated squared deviation of the angular distribution

$$\rho = \int_0^{2\pi} (F(\theta) - \langle F \rangle)^2 d\theta \quad (11)$$

indicates the localization of the probability density around some distinguished angles. The formulae (10) and (11) can be directly applied to analyze an eigenstate φ_n of the quantum billiard. Large value of the factor ρ_n shows that the state ϕ_n is scarred. Moreover, the shape of the angular distribution $F_n(\theta)$ facilitates the correct identification of the periodic orbit responsible for the detected scars. Note, however, that the precision of this method is limited. The scars - concentrations of the probability density along the periodic orbit, have a finite width (depending on the eigenenergy) what causes broadening of the peaks in the angular distribution and complicates their interpretation. For eigenstates corresponding to higher levels

the widths of the scars decrease but the periodic orbits become more complicated and consist of a larger number of segments. It causes an increase of the number of peaks in the angular distribution $F(\theta)$ so some of them may overlap.

5. Pseudo-integrable quantum billiards

Since it is not possible to get analytically the levels and eigenmodes of the quantized pseudointegrable billiards one is left with the numerical methods developed for quantum chaotic billiards [45,22]. As a simple example of the pseudointegrable billiard we have taken the symmetric gnomon depicted in Fig. 8(a). This system, also called “L - shape” billiard, has the classical phase space of genus 2. This becomes clear after inquiring the manifold R represented in Figs 8(b) and 8(c). It consists of four copies of the original billiard. Identifying the corresponding opposite sides, as denoted in Fig. 8(c), one obtains a pretzel with two holes indeed. The autocorrelation function for the classical L-billiard was investigated by Henyey and Pomphrey [37] while its quantum analogue has been studied by Richens and Berry [22].

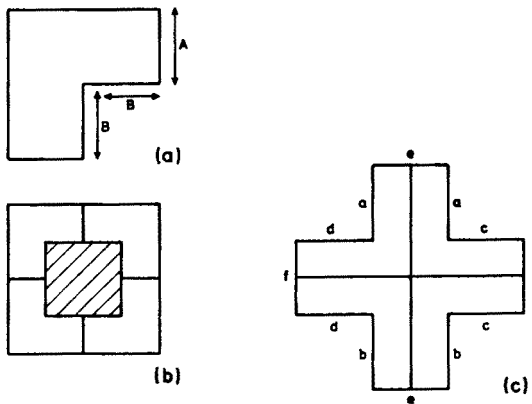


Fig. 8. Schematic picture of the billiard investigated (a); polygon R equivalent to the corresponding invariant surface (b).

Every space reflection symmetry divides eigenstates of a quantum system into two parity classes. Studying the spectral properties of a system it is necessary to consider each class separately [8]. Applying the numerical technique presented in [22] we obtained about 3000 levels for the antisymmetric parity class of the quantum L-billiard [83]. In order to avoid missing some

eigenvalues the total number of levels evaluated was compared with the prediction of the Weyl formula [48]. Since each half of the symmetric gnomon, i.e. the trapeze $(\pi/2, \pi/2, \pi/4, 3\pi/4)$, has the phase space with the same topological properties we may expect that both parity classes (symmetric, with Neumann boundary conditions along the symmetry line or antisymmetric, with the Dirichlet boundary conditions) have similar statistics of the level spacing.

Let A denotes the length of each arm of the billiard and B its width — see Fig. 8(a). We constructed a family of billiards of the same area $S = B^2 + 2AB = 8\pi$, to ensure the mean spacing for each parity classes equal to unity. The level spacing distribution occurred to be almost independent on the shape of the L billiard in a wide range of the parameter A . Also the rationality of the number A/B , which plays an important role in the classical dynamics [23], seems not to influence the character of the distribution $P(s)$ in quantum billiard [83]. The level spacing distribution does not depend on the energy itself. The statistical analysis done separately for the highest quarter of the energy range coincides, within the statistical error, with the statistics obtained for the lowest levels.

A typical numerical results of the level spacing distribution obtained for $A = 8$ are presented in Fig. 9. Note that the probability of level degeneration in the system is negligible and the level repulsion characteristic to classically chaotic systems is observed. This fact requires a comment, inasmuch as the pseudointegrable L-billiard is not chaotic. The source of the pseudo integrability — a corner in the enclosure of the billiard can not induce chaos into the classical dynamics. The set of trajectories hitting the corner is of measure zero. As discussed in the preceding section a single classical periodic orbit can essentially affect the global properties of the quantum system. In a similar manner one singular point in the boundary of the billiard may modify the Poisson spectrum of a regular system.

The numerical results presented in the histogram in figure 9 do not coincide, however, to the GOE distribution (or to the Wigner surmise) typical to classically chaotic systems [50]. The distribution resulting from the additive random matrices (7) might be used instead [66]. Best fit obtained for $\lambda = 0.38$ is represented by the bold line in the picture. The simple model of additive matrices is useful to describe the level statistics of pseudointegrable system. One might interpret the coupling between two tori in the classical phase space as the perturbation G in Eq. (7) changing the properties of the Poisson term H_0 corresponding to the regular motion on a torus. On the other hand the quality of the fit is not excellent and suggests that the employed distribution can only be regarded as a rough approximation of the results obtained.

Numerical results for $P(s)$ are similar for all the shapes of L-billiard

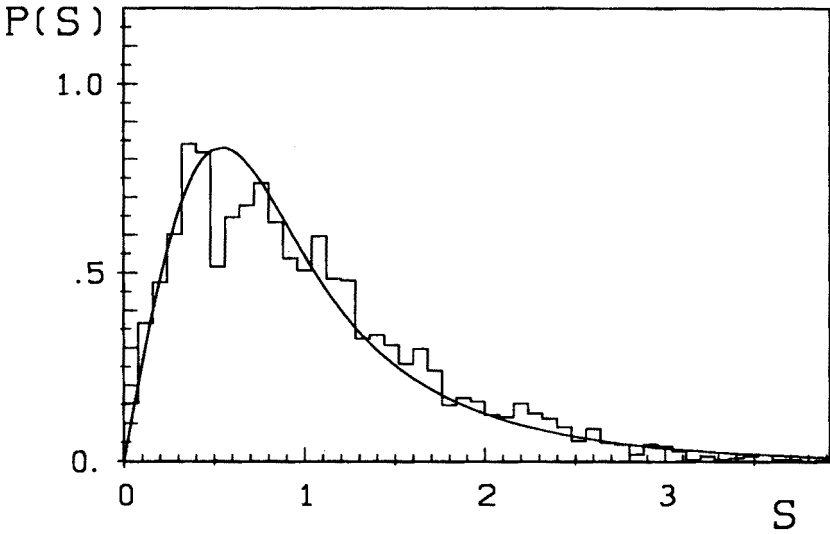


Fig. 9. Level spacing distribution $P(s)$ for the first 2673 levels of the antisymmetric parity class of the L-shape billiard with $A = 8.0$. Best fit of the additive random matrices with $\lambda = 0.38$.

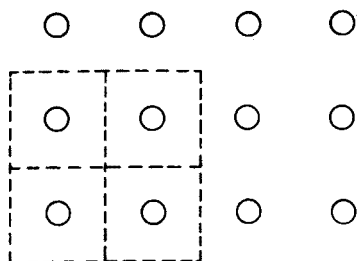
considered (excluding the limiting cases of $A \rightarrow 0$ and $A \rightarrow \infty$). It might be therefore tempting to speculate that the level statistics of the pseudo-integrable quantum billiards is determined only by the genus of its invariant surface. Some preliminary results of the level distribution for other quantum pseudointegrable systems of genus 2 seem to support this conjecture. Shudo and Shimizu studied the quantum billiards in pseudointegrable triangles of genus 2 (right triangles with vertex angle α equal to $\pi/4$ or $\pi/5$ or $2\pi/5$) and reported [84] similar properties of $P(s)$. Šeba gave another example of the genus 2 billiard introducing a singular point interaction [40]. Shrinking the radius of the circular obstacle in the Sinai billiard to zero one gets a pseudointegrable system. Its level spacing distribution displays characteristic linear level repulsion with the slope different as this typical to chaotic systems [85]. Comparable results were recently reported [86,87] for other pseudointegrable billiards with singular perturbation.

Up to now we discussed the theoretical studies of the quantized billiards. An interesting complementary picture provide recent experiments performed with microwave resonators. Stöckmann and Stein [24] transmitted the microwaves through thin metallic resonators of different shapes and measured the absorption spectra. Since the Schrödinger equation of quantum billiard is equivalent to the Helmholtz equation (4) describing the microwaves in 2 dimensional resonator, the observed absorption dips correspond to eigenvalues of the billiard. The level statistics for the resonator

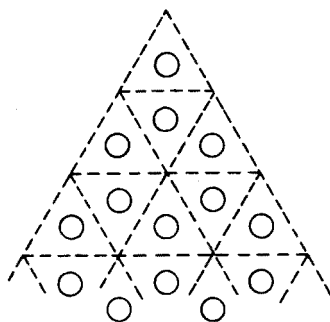
in shape of Sinai billiard fits well [24] to the expected Wigner distribution (6). The thin antenna, used to transport microwaves into resonator, may be regarded as a point interaction and influences the measured spectrum. Experimental results of level spacing distribution obtained for rectangular resonator [25] are resembling these presented in Fig. 9, which are received for pseudointegrable billiard of genus 2.

6. Quantum chaotic scattering

The classical dynamics of the Sinai billiard is equivalent to the behaviour of a point particle bouncing in an infinite lattice of the circular elastic scatterers represented in Fig. 10(a). Its dependence on the radius of scatterers R is given in [88]. Analogically, the equilateral triangular billiard with the circular obstacle, corresponds to the scattering in an infinite periodic hexagonal lattice — see Fig. 10(b).



(a)



(b)

Fig. 10. Scattering billiard systems: (a) Sinai billiard gives the rectangular lattice; (b) circular obstacle in equilateral triangle leads to the hexagonal lattice.

In addition to investigation of the bounded systems (or infinite lattices) it is interesting and instructive to study simple open systems consisting

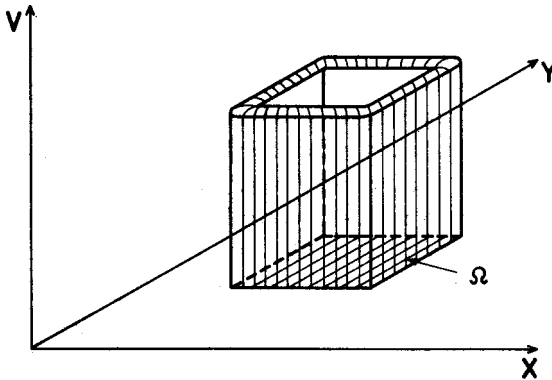


Fig. 11. Model of the billiard with penetrable walls suitable for study of chaotic scattering.

of three [27,89] or four [90,91] reflecting disks. The classical scattering in such systems is highly unstable and chaotic: the final direction of outgoing trajectory depends strongly on the incoming angle and angular momentum (measured respectively the center between disks). This classical feature manifest itself in the corresponding quantum system. Differential cross section $d\sigma/d\theta$ oscillates with the angle θ and the total cross section σ displays erratic fluctuations as a function of energy [90,92]. Similar effects occur in problems of quantum scattering not only on hard reflective walls of the billiards [27,90], but likewise on soft [93-95] or singular [96,97] potentials and are the subject of a considerable interest.

Consider a two dimensional billiard with hard impenetrable walls encircling the compact set Ω . In addition to study the bounded quantum problem *inside* Ω one may analyze the open scattering problem *outside* the set Ω . It is known that these two models are related [92]: a chaotic dynamics inside the billiard leads to the irregular scattering outside. Both problems might be directly coupled by making the walls of the billiard penetrable. Walls with finite height and width complicate the analysis, since a resonant phenomena connected with the finite width of the walls appear. It is therefore advantageous to consider the limit of very thin walls and to discuss a model defined by a singular potential [98]

$$V(x, y) = \begin{cases} 0, & \{x, y\} \notin \partial\Omega \\ \frac{1}{\gamma} \delta(x, y), & \{x, y\} \in \partial\Omega \end{cases} \quad (12)$$

where $\partial\Omega$ is the boundary of the billiard and γ is a coupling constant. A scheme of this system is shown in Fig. 11. For zero coupling constant the walls are not penetrable and one encounters two separate systems.

In the case of a positive value of the coupling parameter γ the wave packet can penetrate the walls of the billiard. The resulting scattering system may be described in the S matrix formalism [99]. The long living quasistationary states (resonances) are represented by the complex poles ($z = E - i\varepsilon$) of the analytically continued Green's function. For $\gamma = 0$ the poles are located on the real energy axes and represent the eigenvalues of the bounded billiard. With nonzero coupling constant they lay in the lower part of the complex energy plane. The real part of the pole determines the energy of the corresponding resonance and the imaginary part its width. For small γ all resonances are narrow and well separated. The average width (ε) grows with γ and the resonances start to overlap. Due to this fact the dependence of the total cross-section on energy becomes complicated [100]. This feature is known in the theory of nuclear reactions as the *Ericson fluctuations* [101].

It is interesting to analyze the statistical properties of the resonant poles on the complex plane. In the case of a weak coupling the poles are localized close to the real axis and the statistics of spacing between neighbouring resonances reveals the dynamics of the classical billiard in the set Ω . For chaotic billiards the Wigner distribution is expected. The statistics of the resonance widths ε is given in this case by the Porter-Thomas distribution [55]. Large value of the coupling constant γ causes spreading of the poles far into the lower half of the complex energy plane. It is then useful to study the distribution of the distances (in the two dimensional Euclidean metric) between closest poles. The Poisson process on the plane (uncorrelated random points uniformly drawn on the plane) the next neighbour distribution is given [8] by the Wigner formula (6) characterized by the linear point repulsion. On the other hand, the statistics of poles of the chaotic billiard with transparent walls displays cubic repulsion $P(s) \sim s^3$ [97,100]. Similar results were recently obtained for the distribution of complex quasienergies of a periodically kicked system with dissipation [102] and may be well approximated by the distribution of the 2×2 Ginibre ensemble [103]

$$P_G(s) = 2(9\pi/16)^2 s^3 \exp(-9\pi s^2/16). \quad (13)$$

The statistical study of an open quantum system consists also on an analysis of the properties of the unitary scattering matrix S . It has been conjectured [28,90] that the S matrix of a system displaying chaotic irregular system can be described by the Dysons *circular orthogonal ensemble* (COE) [104]. Several features of the distribution of the eigenphases of a COE member on the unit circle are comparable to the corresponding characteristics of the level distribution of GOE matrix [55]. In particular the spacing distributions are the same for both ensembles and are well approximated by the Wigner surmise [8]. This property the S matrix has been checked by

Blümel and Smilansky for a system consisting of a periodic array of scattering discs [105]. In agreement to the predictions of the random matrix theory [55] the statistics of the squared moduli of the elements $y = |S_{mn}|^2$ was found to be Poissonian. Both statistics $P(s)$ and $P(y)$ are different, if the corresponding classical dynamics is regular [105], and thus are helpful in studying the quantum chaotic scattering. It has to be noted, however, that also non chaotic systems with COE like S matrix are known [106].

7. Concluding remarks

After many years of intensive studies several aspects of the dynamics of classical billiards are well understood. In particular a general definition of chaotic billiard (with positive Kolomogorov entropy) is established [1,31]. Some classical billiards are shown to be chaotic [3,4,33-36], but there are still no universal methods allowing to state, whether the billiard in a given two dimensional enclosure is chaotic.

Not so much is known about the corresponding quantum billiards, since up to now no precise definition of quantum chaos has been formulated [5,107]. One is left with an phenomenological approach analyzing various features of quantum systems [8]. It has been conjectured [50] and later confirmed in series of numerical experiments [51,107] that quantum analogues of classically chaotic systems display spectral fluctuations properly described by ensembles of random matrices [54]. Several statistics quantitatively measuring the properties of spectrum of the quantum system allow to determine the nature of the corresponding classical dynamics. As a simple example let us mention the level spacing distribution $P(s)$: it reveals the level clustering for generic integrable systems and the level repulsion for classically chaotic billiards.

A particular class of classical pseudointegrable systems, with the phase space of genus $g > 1$, possess some properties of both categories and may be regarded as an intermediate case. Classical pseudointegrable billiards are not chaotic (zero Kolomogorov entropy), but their quantum counterparts exhibit level repulsion. The level statistics differs, however, from the GOE distribution typical to classically chaotic billiards. We conjecture that the level spacing distribution of a quantum billiard depends solely on the genus g of the corresponding classical phase space.

Moreover, the level spacing distribution $P_g(s)$, universal for all billiards with genus g , approaches the Wigner surmise (6) (more precisely, the GOE distribution) in the limiting case

$$\lim_{g \rightarrow \infty} P_g(s) = P_W(s). \quad (14)$$

It is possible to find in the literature arguments supporting this thesis. Cheon and Cohen considered the approximation of the Sinai billiard by a N -steps stair-like billiard [108]. The level statistics for this quantum system of genus N becomes very close to the GOE predictions already for $N = 6$. Further, Shudo and Shimizu analyzed the quantized rhombus billiard with an irrational angle α , what corresponds to the case of $g \rightarrow \infty$ [84]. Although this system does not display the classical chaos (Lyapunov exponents vanish), its quantum analogue shows level statistics very close to the GOE distribution, characteristic to quantized chaotic systems.

However, the above conjecture can not be valid without restrictions. Dittrich and Smilanski have shown [109] that the classically chaotic composite billiard consisting of several cavities coupled by narrow holes displays the Poissonian level statistics. This is due to the dynamical localization or, in other words, due to superposition of several independent Wigner spectra. The same reasoning might be applied to the elongated pseudointegrable billiards, so the statement (14) is not valid for composite systems where localization occurs. Furthermore, in the limiting case of large integers N , the pseudointegrable billiard of genus N approximating the chaotic Sinai billiard displays different properties than the billiard of the same genus approximating the integrable system.

The level distribution of quantum pseudointegrable systems confirms the hypothesis that the singular points in the billiards boundary of measure zero strongly influence the quantum dynamics. In a similar matter classical periodic orbits generate quantum scars — ordered structures existing for some eigenstates of the quantized chaotic billiards [13-15]. This phenomenon is already understood to some extent [77-79], but the recently developed semiclassical theory of scarring [16,17] is not capable to predict what eigenstates are scarred by what periodic orbit. In spite of a considerable effort [18,89,110-113] it is not yet clear how precisely the classical periodic orbits determine the density of the spectrum of the corresponding quantum system.

Billiard with penetrable walls may serve as a model open system suitable to study properties of quantum scattering [98]. The statistical approach is successful also in this case. The distribution of the complex poles of the S matrix [97] or the statistics of the eigenphases of the unitary matrix S [105] allows to distinguish between regular and chaotic scattering. For a classically chaotic billiard Ω the open system, defined by potential (12), leads to the scattering matrix S well described by the theory of random matrices [53-55,104]. However, the properties of scattering system build of a pseudointegrable billiard Ω have not been investigated in detail. In general it would be interesting to investigate, in what manner the pseudo integrability of a classical system and the topology of the phase space affect

the fundamental properties of the quantum analogue, studying for example, the quantum propagators obtained from the classical trajectories.

A further work is also needed to elucidate the role of quantum scars in chaotic scattering. One might expect that some resonances, corresponding to scarred eigenstates of the bounded billiard, are influenced by classical periodic orbits. This leads to the specific behaviour of the angular dependence of the differential cross section.

Special thanks are due to Petr Šeba for fruitful collaboration on pseudo-integrable systems and to Stefan Thomae, who encouraged me to study classical billiards. I have also benefited from numerous discussions with A. Csordas, M. Feingold, F. Haake, G. Lenz, J. Stein and H-J. Stöckmann. The travel grant from Fundacja Stefana Batorego is gratefully acknowledged.

REFERENCES

- [1] B.V. Chirikov, *Phys. Rep.* **52**, 265 (1979).
- [2] A.J. Lichtenberg, M.A. Lieberman, *Regular and Stochastic Motion*, Springer, Berlin 1983.
- [3] Ya.G. Sinai, *Introduction to Ergodic Theory*, Princeton University Press, Princeton, 1976.
- [4] L.A. Bunimovich, *Math. USSR Sb.* **23**, 45 (1974).
- [5] G. M. Zaslavski, *Phys. Rep.* **80**, 157 (1981).
- [6] T. Yukawa, T. Ishikawa, *Progr. Theor. Phys. Suppl.* **98**, 157 (1989).
- [7] M.V. Berry, M. Tabor, *Proc.R.Soc.London.* **A356**, 375 (1977).
- [8] F. Haake, *Quantum Signatures of Chaos*, Springer, Berlin 1991.
- [9] M.V. Berry, *Ann. Phys.* **131**, 163 (1981).
- [10] T. Ishikawa, T. Yukawa, *Phys. Rev. Lett.* **54**, 1617 (1985).
- [11] A. Shudo, Y. Shimizu, *Phys. Rev. A* **42**, 6264 (1990).
- [12] S.W. McDonald, A.N. Kaufmann, *Phys. Rev. Lett.* **42**, 1189 (1979) and *Phys. Rev.* **A37**, 3067 (1988).
- [13] E.J. Heller, *Phys. Rev. Lett.* **53**, 1515 (1984).
- [14] E.J. Heller, P.W. O'Connor, J. Gehlen, *Phys. Scr.* **40**, 354 (1989).
- [15] E.B. Bogomolny, *Physica* **31D**, 169 (1988).
- [16] M.V. Berry, *Proc. R. Soc. London* **A423**, 219 (1989).
- [17] M. Feingold, R.G. Littlejohn, S.B. Solina, J.S. Pehling, O. Piro, *Phys. Lett.* **A146**, 199 (1990).
- [18] M.C. Gutzwiller, *J. Math. Phys.* **12**, 343 (1971).
- [19] A.M. Ozorio de Almeida, *Hamiltonian Systems: Chaos and Quantization*, Cambridge University Press, 1988.
- [20] M.V. Berry *Proc. R. Soc. London* **A400**, 229 (1985).
- [21] A.N. Zemlyakov, A.B. Katok, *Math. Notes* **18**, 291 (1975).
- [22] P.J. Richens, M.V. Berry, *Physica* **2D**, 495 (1981).

- [23] E. Gutkin, *Physica* **19D**, 311 (1986).
- [24] H.-J. Stöckmann, J. Stein, *Phys. Rev. Lett.* **64** 2215 (1990).
- [25] F. Haake, G. Lens, P. Šeba, J. Stein, H.J. Stöckmann and K. Życzkowski, *Phys. Rev.* **A44**, R6161 (1991).
- [26] B. Eckhardt, *Physica* **D33**, 89 (1988).
- [27] P. Gaspard, S. Rice, *J. Chem. Phys.* **90**, 2225 (1989).
- [28] R. Blümel, U. Smilansky, *Phys. Rev. Lett.* **64**, 241 (1990).
- [29] W. Thirring *Classical Dynamical Systems*, Springer, New York, 1977.
- [30] Ya.G. Sinai, *Russ. Math. Surv.* **25**, 137 (1970).
- [31] J.P. Kronfeld, Ya.G. Sinai, S.V. Fomin, *Ergodic Theory*, Nauka, Moscow, 1980.
- [32] V.F. Lazutkin, *Math. USSR Izv.* **37**, 186 (1973).
- [33] L.A. Bunimovich, *Comm. Math. Phys.* **65**, 295 (1979).
- [34] M. Wojtkowski, *Comm. Math. Phys.* **105**, 391 (1986).
- [35] R. Markarian, *Comm. Math. Phys.* **118**, 87 (1988).
- [36] L.A. Bunimovich, *Physica* **33D**, 58 (1988).
- [37] F.S. Henyey, N. Pomphrey, *Physica* **6D**, 78 (1982).
- [38] B. Eckhardt, J. Ford, F. Vivaldi, *Physica* **13D**, 339 (1984).
- [39] J.H. Hannay, R.J. McCraw, *J. Phys.* **A23**, 887 (1990).
- [40] P. Šeba, *Phys. Rev. Lett.* **64**, 1855 (1990).
- [41] B. Mirbach, H.J. Korsch, *Nonlinearity* **2**, 327 (1989).
- [42] M.V. Berry, M. Wilkinson, *Proc. R. Soc. London* **A392**, 15 (1984).
- [43] C.G. Jung, *Can. J. Phys.* **58**, 719 (1980).
- [44] G. Casati, I. Guarneri, *Phys. Rev. Lett.* **54**, 1350 (1985).
- [45] R.J. Riedell, *J. Comput. Phys.* **31**, 21 (1979).
- [46] M. Toda, K. Ikeda, *Phys. Lett.* **A124**, 165 (1987).
- [47] F. Haake, H. Wiedemann, K. Życzkowski, to be published.
- [48] H.P. Baltes, E.R. Hilf *Spectra of Finite Systems*, B-I. Wissenschaftsverlag, Mannheim, 1978.
- [49] G. Casati, F. Valz-Gris, I. Guarneri, *Lett. Nuovo Cimento* **28**, 279 (1980).
- [50] O. Bohigas, M.J. Giannoni, C. Schmit, *Phys. Rev. Lett.* **52**, 1 (1984).
- [51] T. Yukawa, T. Ishikawa, *Progr. Theor. Phys. Suppl.* **98**, 157 (1989).
- [52] D.K. Siegwart, *J. Phys. A* **22**, 3537 (1989).
- [53] C.E. Porter, *Statistical Theory of Spectra*, Academic Press, 1965.
- [54] M.L. Mehta, *Random Matrices*, 2 ed. Academic Press, 1990.
- [55] T.A. Brody, J. Flores, J.B. French, P.A. Mello, A. Pandey, S.S.M. Wong, *Rev. Mod. Phys.* **53**, 385 (1981).
- [56] M.L. Mehta, J. Des Cloiseaux, *Indian J. Math* **3**, 329 (1971).
- [57] B. Dietz, F. Haake, *Z. Phys.* **B80**, 153 (1990).
- [58] B. Dietz, K. Życzkowski, *Z. Phys.* **B84**, 157 (1991).
- [59] M. Robnik, M.V. Berry, *J. Phys. A* **18**, 1361 (1985).
- [60] M.V. Berry, M. Robnik, *J. Phys. A* **19**, 649 (1986).
- [61] M. Kuś, R. Scharf, F. Haake, *Z. Phys.* **B66**, 129 (1987).
- [62] K. Nakamura, H. Thomas, *Phys. Rev. Lett.* **61**, 247 (1988).
- [63] M.V. Berry, M. Robnik, *J. Phys. A* **17**, 2413 (1984).
- [64] T. Cheon, *Phys. Rev.* **A42**, 6227 (1990).

- [65] G. Lenz, F. Haake, *Phys. Rev. Lett.* **65**, 2325 (1990).
- [66] G. Lenz, K. Życzkowski, D. Saher, *Phys. Rev.* **A44**, (1991) 8043 (1991).
- [67] T.A. Brody, *Lett. Nuovo Cimento* **7**, 482 (1973).
- [68] H. Hasegawa, H.J. Mikeska, H. Frahm, *Phys. Rev.* **A38**, 395 (1988).
- [69] M. Robnik, *J. Phys. A* **20**, L495 (1987).
- [70] F. Izrailev, *Phys. Rep.* **196**, 299 (1990).
- [71] F.J. Dyson, M.L. Mehta, *J. Math. Phys.* **4**, 701 (1963).
- [72] A. Pandey, *Ann. Phys. NY* **119**, 170 (1979).
- [73] M.V. Berry, *Proc. R. Soc. London* **A400**, 229 (1985).
- [74] M.V. Berry, *Nonlinearity*, **1**, 399 (1988).
- [75] M. Shapiro, G. Goelman, *Phys. Rev. Lett.* **53**, 1714 (1984).
- [76] R. Aurich, F. Steiner, *Physica* **D48**, 445 (1991).
- [77] P. Leboeuf, A. Voros, *J. Phys. A* **23**, 1765 (1990).
- [78] P.W. O'Connor, S. Tomsovic, *Ann. Phys.* **207**, 218 (1991).
- [79] M. Kuś, J. Zakrzewski, K. Życzkowski, *Phys. Rev.* **A43**, 4244, (1991).
- [80] S. Tomsovic, E.J. Heller, *Phys. Rev. Lett.* **67**, 665 (1991).
- [81] D. Wintgen, A. Hönig, *Phys. Rev. Lett.* **63**, 1467 (1989).
- [82] H. Frisk, *Physica Scripta* **43**, 545 (1991).
- [83] K. Życzkowski, P. Šeba, submitted to *Phys. Lett A*.
- [84] A. Shudo, Y. Shimizu, preprint, Waseda University, Tokyo, 1991.
- [85] P. Šeba, K. Życzkowski, *Phys. Rev.* **A44**, 3457 (1991).
- [86] T. Cheon, T. Mizusaki, T. Shigehara, N. Yoshinaga, preprint Hosei University Tokyo HU-PH-020913TC, 1990.
- [87] C.H. Lewenkopf, *Phys. Rev.* **A42**, 2431 (1990).
- [88] J-P. Bouchaud, P. Le Doussal, *Physica* **D20**, 335 (1986).
- [89] P. Cvitanovic, B. Eckhardt, *Phys. Rev. Lett.* **63**, 823 (1989).
- [90] E. Doron, U. Smilansky, A. Frenkel, *Physica* **D50**, 367 (1991).
- [91] C.W. Beenakker, H. van Houten, *Phys. Rev. Lett.* **63**, 1857 (1989).
- [92] E. Doron, U. Smilansky, preprint Rehovot, WIS 91/63, 1991.
- [93] C. Jung, S. Pott, *J. Phys.* **A23**, 3729 (1990).
- [94] L. Wiesenfeld, *Comm. At. Mol. Phys.* **25**, 335 (1991).
- [95] C. Jung, *Acta Phys. Pol.* (1992) this issue.
- [96] H.R. Jauslin, *Physica* **D51**, 200 (1991).
- [97] W. John, B. Milek, H. Schanz, P. Šeba, *Phys. Rev. Lett.* **67**, 1949 (1991).
- [98] P. Šeba, *Phys. Rev.* **A43**, 2068 (1991).
- [99] A. Messiah, *Quantum Mechanics*, North-Holland, Amsterdam, 1975.
- [100] A. Csordas, P. Šeba, to appear 1992.
- [101] T. Ericson, *Phys. Rev. Lett.* **5**, 430 (1960).
- [102] R. Grobe, F. Haake, *Phys. Rev. Lett.* **62**, 2893 (1989).
- [103] J. Ginibre, *J. Math. Phys. (N.Y.)* **6**, 440 (1965).
- [104] F. J. Dyson, *J. Math. Phys.* **3**, 157 (1962).
- [105] R. Blümel, U. Smilansky, *Physica* **D36**, 111 (1989).
- [106] C.H. Lewenkopf, H.A. Weidenmüller, *Ann. Phys.* **212**, 53 (1991).
- [107] H. Cerdeira ed., *Proceedings of Workshop on Quantum Chaos, Trieste 1990*, World Scientific, Singapore, 1991.

- [108] T. Cheon, T.D. Cohen, *Phys. Rev. Lett.* **62**, 2769 (1989).
- [109] T. Dittrich, U. Smilanski, *Nonlinearity* **4**, 59 (1991).
- [110] A.M. Ozorio de Almeida, M. Saraceno, *Ann. Phys.* **210**, 1 (1991).
- [111] M. Sieber, F. Steiner, *Phys. Rev. Lett.* **67**, 1941 (1991).
- [112] G. Tanner, P. Scherer, E.B. Bogomolny, B. Eckhardt, D. Wintgen, *Phys. Rev. Lett.* **67**, 2410 (1991).
- [113] P. Dahlqvist, G. Russberg, *J. Phys. A* **24**, 4763 (1991).